6. D. R. Nelson and L. Peliti, *J. Phys. (Paris)* **48**, 1095 (1987); J. A. Aronovitz and T. C. Lubensky, *Phys. Rev. Lett.* **60**, 2634 (1988).
7. C. Y. Young, R. Pindak, N. A. Clark, R. B. Meyer, *Phys. Rev. Lett.* **40**, 773 (1978); D. E. Moncton and R. Pindak, *ibid.* **43**, 701 (1979).
8. E. B. Sirota, P. S. Pershan, L. B. Sorensen, J. Collett, *Phys. Rev. A* **36**, 2890 (1987).
9. J. D. Brock *et al.*, *Phys. Rev. Lett.* **57**, 98 (1986).
10. DMPC, >99% pure, obtained from Avanti Polar Lipids, Birmingham, AL.
11. D. Wack and W. W. Webb, *Phys. Rev. Lett.* **61**, 1210 (1988).
12. J. A. N. Zasadzinski, J. Schneir, J. Gurley, V. Elings, P. K. Hansma, *Science* **239**, 1013 (1988).
13. G. S. Smith, E. B. Sirota, C. R. Safinya, N. A. Clark, *Phys. Rev. Lett.* **60**, 813 (1988).
14. R. E. Peierls, *Helv. Phys. Acta Suppl.* 7, 81 (1934).
15. L. D. Landau, in *Collected Papers of L. D. Landau*, D. Ter Haar, Ed. (Gordon & Breach, New York, 1965), p. 209.
16. A. Caille, *C. R. Acad. Sci. Ser. B* **274**, 891 (1972).
17. J. Als-Nielsen *et al.*, *Phys. Rev. B* **22**, 312 (1980).
18. C. R. Safinya, E. B. Sirota, D. Roux, G. S. Smith, in preparation.
19. We acknowledge helpful conversations with D. Roux and S. K. Sinha and the technical assistance of R. Hewitt, M. Sansone, and K. D'Amico. Part of this work was done at the Stanford Synchrotron Radiation Laboratory and at the National Synchrotron Light Source (Brookhaven), which are funded by the Department of Energy. Part of this research was supported by joint Industry-University NSF grant DMR-8307157.

7 July 1988; accepted 30 September 1988

Neonatal Hepatitis Induced by α_1-Antitrypsin: A Transgenic Mouse Model

MARK J. DYCAICO, SETH G. N. GRANT, KATHERINE FELTS, W. STEPHEN NICHOLS, STEPHEN A. GELLER, JEFFREY H. HAGER, AMY J. POLLARD, STEVEN W. KOHLER, HEIDI P. SHORT, FRANK R. JIRIK, DOUGLAS HANAHAN, JOSEPH A. SORGE*

Transgenic mouse lineages were established that carry the normal (M) or mutant (Z) alleles of the human α_1-antitrypsin (α_1-Pi) gene. All of the α_1-Pi transgenic mice expressed the human protein in the liver, cartilage, gut, kidneys, lymphoid macrophages, and thymus. The human M-allele protein was secreted normally into the serum. However, the human Z-allele protein accumulated in several cell types, but particularly in hepatocytes, and was found in serum in tenfold lower concentrations than the M-allele protein. Mice in one lineage carrying the mutant Z allele expressed high levels of human α_1-Pi RNA and displayed significant runting (50% of normal weight) in the neonatal period. This lineage was found to have α_1-Pi–induced liver pathology in the neonatal period, concomitant with the accumulation of human Z protein in diastase-resistant cytoplasmic globules that could be revealed in the Periodic acid–Schiff reaction (PAS). The phenotype of mice in the strain expressing high levels of the Z allele is remarkably similar to human neonatal hepatitis, and this strain may prove to be a useful animal model for studying this disease.

THE α_1-PROTEASE INHIBITOR (α_1-antitrypsin; α_1-Pi) is a serum protein that inhibits trypsin, elastase, thrombin, chymotrypsin, factors XI and XIII, and plasmin. Its major physiologic function is to inhibit neutrophil elastase, providing 90% of the antielastase activity of serum (*1*). Individuals with α_1-Pi deficiency are at an increased risk of developing emphysema, usually in the fourth to fifth decades of life. The lung pathology results from the destruction of alveolar walls, presumably because of the unchecked activity of neutrophil elastase.

Genetically, α_1-Pi deficiency is autosomal and expressed in a codominant pattern. Approximately 100,000 individuals in the United States have clinical α_1-Pi deficiency. The most common alleles of the gene are designated as Pi^M (normal, with a gene frequency of 0.95), Pi^S (0.03), and Pi^Z (0.02). The MM, ZZ, and MZ phenotypes are associated with serum α_1-Pi levels of 2, 0.3, and 1.2 mg/ml, respectively.

The protein itself has a molecular size of 53 kD with three or four carbohydrate side chains. Its major site of synthesis is the liver. The S mutant contains a valine instead of a glutamic acid at amino acid position 264. The Z mutant contains a lysine instead of a glutamic acid at position 342 (*2, 3*). The Z mutation does not affect the amount of protein synthesized by the liver nor the ability of the protein to inhibit proteases, but rather affects the transport of the protein across the rough endoplasmic reticulum of liver cells. Liver histology of ZZ patients typically reveals diastase-resistant PAS-positive globules in the periportal hepatocytes (*4*), reflecting the buildup of the protein as a result of the transport defect. The transport mechanism in the endoplasmic reticulum is not known.

Approximately 15% of neonates with the ZZ genotype develop hepatitis; 25% of these develop obstructive jaundice and cirrhosis, and eventually die before age 8 (*5*). The pathophysiology has been attributed to intracytoplasmic inclusions of α_1-Pi within hepatocytes (*6*). It is suspected that neonates with hepatitis are more likely to develop cirrhosis as adults. It is not known why only 15% of ZZ homozygotes develop hepatitis, although it has been suggested that increased liver damage in these individuals is caused by expression of higher levels of protein in liver cells. It is also not known why boys develop α_1-Pi hepatitis more often than girls by a 2:1 ratio. In adults, liver disease associated with α_1-Pi is seen primarily in the form of cirrhosis. About 17% of all adults with nonalcoholic cirrhosis have the MZ heterozygous genotype (*7*). Again, there is a 2:1 ratio of male to female α_1-Pi patients with nonalcoholic cirrhosis.

To study the effects of human α_1-Pi alleles, transgenic mice were produced that contain the human α_1-Pi M and Z genes. To increase the probability of regulated, high-level expression, genomic λ clones that contained a substantial amount of 5′ flanking region were isolated (Fig. 1). A Sna B1–Eco RI fragment (6.1 kb) of the λ clone containing the M allele was exchanged with the same length fragment from a clone containing the Z mutation located in exon G (Fig. 1). Thus two clones, each containing 21.4 kb of human α_1-Pi sequence, were produced that differed at a single nucleotide responsible for the Z mutation. The presence of the Z mutation was confirmed by nucleotide sequencing.

The 21.4-kb Sal I fragments were gel purified and injected into fertilized F2 mouse embryos derived by intercrossing B6D2F1/J (C57BL/6J × DBA/2J) mice (*8*).

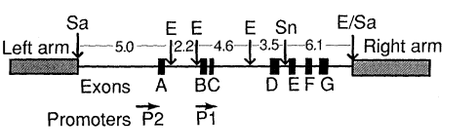

Fig. 1. Map of the human α_1-Pi genomic clone used to construct transgenic animals. Exons A and B and the macrophage-specific promoter (P_2) have recently been discovered (*17*); exon C was originally referred to as exon 1. P_1 is the hepatocyte-specific promoter. The distances between restriction sites are in kilobases. Genomic libraries were constructed in λ EMBL-3 from normal human DNA and from cell line GM3578, which is homozygous for the α_1-Pi Z allele. E, Eco RI, Sa, Sal I, Sn, Sna BI.

M. J. Dycaico, K. Felts, A. J. Pollard, S. W. Kohler, H. P. Short, F. R. Jirik, J. A. Sorge, Stratagene, La Jolla, CA 92037.
S. G. N. Grant, J. H. Hager, D. Hanahan, Cold Spring Harbor Laboratories, Cold Spring Harbor, NY 11724.
W. S. Nichols and S. Geller, Department of Pathology and Laboratory Medicine, Cedars Sinai Medical Center, Los Angeles, CA 90048.

*To whom correspondence should be addressed.

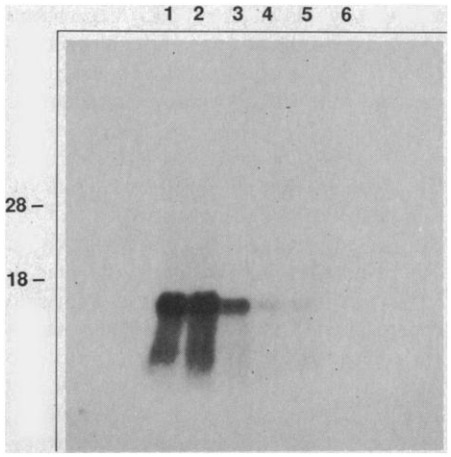

Fig. 2. A formaldehyde-RNA blot (*18*) of 20 μg each of total liver RNA isolated from transgenic hemizygote lineages. Lane 1, M#1; lane 2, Z#2; lane 3, M#2; lanes 4 and 5, Z#1; lane 6, a nontransgenic control mouse. The RNA blot was probed with human α_1-Pi ^{32}P-labeled DNA probe specific to exon D.

Seven transgenic founder animals were produced with the M and Z human alleles. Two lines for each allele were bred to create lineages (M#1, M#2, Z#1, and Z#2) to allow further analyses (*9*). It was estimated that the human α_1-Pi DNA copy numbers for lineages M#1, M#2, Z#1, and Z#2 were approximately 25, 5, 5, and 12 copies per haploid mouse genome, respectively (*10*).

To determine if any of the transgenic animals were producing human α_1-Pi RNA, an RNA blot of total liver RNA was performed (Fig. 2). The transgenic mice all showed evidence of expression, with the highest levels of RNA in the M#1 and Z#2 lineages. Although lineage Z#2 produced more α_1-Pi RNA in the liver than M#2, its level of protein in the serum was considerably less (Fig. 3). An enzyme-linked immunosorbent assay (ELISA) indicated that the two M lineages produced significantly higher levels of serum protein than the Z lineages (*10*). The level of α_1-Pi in human serum is typically 2.0 mg/ml. The M#1 lineage accumulated serum levels of 7 mg/ml; the M#2 lineage accumulated approximately the same serum levels as in humans. However, Z lineage #2 accumulated 0.6 mg of human α_1-Pi per milliliter of serum, even though Z#2 expressed as much α_1-Pi RNA in the liver as M#1, and Z#1 accumulated 0.3 mg of human α_1-Pi per milliliter of serum. This is consistent with a transport defect in liver cells, as is the case in the human Z-allele disease. This result also suggests that the mechanism responsible for impaired transport of the Z mutant protein is not species specific.

Four of 11 offspring from a Z#2 × B6CBA F1 litter appeared small compared with their littermates (7 versus 14 g at 3 weeks of age). Upon analysis of the tail blots, the four smaller animals were found to be positive for the transgene whereas the seven larger animals did not carry the transgene. All offspring from intercross matings within the M#1, M#2, and Z#1 inbred lineages were normal in size and weight. However, offspring from intercross matings of Z#2 hemizygotes displayed unusual characteristics. The litters typically contained six to eight pups. Frequently pups would die in the first 2 weeks of life. However, particularly in litters of which there was little or no death, even smaller animals were observed. At 3 weeks of age, some transgenic animals weighed as little as 4 g whereas the normal animals weighed approximately 14 g. We bred some of these smaller transgenic animals (4 g at 3 weeks) with nontransgenic animals to determine if these animals were homozygous for the transgene. Only one out of three animals was fertile, and it was heterozygous. We also outbred nine of the larger Z#2 transgenic animals (7 g at 3 weeks) with nontransgenic animals and again found no homozygotes. To date, we have been unable to identify a homozygous Z#2 animal. Figure 4 shows the average weight of ten Z#2 transgenic animals against the average weight of ten normal littermates. Over a period of 3 months, the transgenic animals began to gain weight and reached nearly normal size.

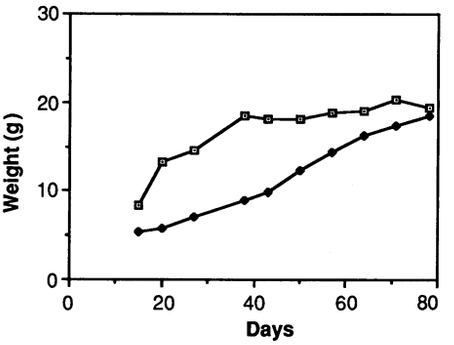

Fig. 4. Growth curves for normal and Z#2 transgenic mice averaged for ten animals in each category. Open squares, normal; closed diamond, Z#2.

Normal mouse liver sections, stained with hematoxylin-eosin (H-E), showed intact lobular architecture and only a sparse lymphocytic accumulation within portal tracts. Intracytoplasmic inclusions were not demonstrable with the Periodic acid–Schiff reaction after diastase digestion (dPAS) or with rabbit antiserum to α_1-Pi and the peroxidase–anti-peroxidase (PAP) method. Other organs in normal mice, including brain, heart, lung, thymus, spleen, lymph node, stomach, small intestine, pancreas, kidney, ovary, adrenal, salivary gland, striated muscle, and skin were unremarkable.

The morphologic changes seen in the tissues from transgenic mice varied according to the allele injected and level of RNA expression; histologic phenotypic expression was more marked in the Z lineages than in the M. The livers of the M-lineage mice were marked by slight lobular disarray as a result of an irregular increase in size of hepatocytes. Most of the hepatocytes contained coarsely granular basophilic cytoplasmic material, consistent with hypertrophied endoplasmic reticulum. Some of the hepatocytes were binucleate or contained enlarged and hyperchromatic nuclei. Neither intracytoplasmic granules nor globules were seen after dPAS reaction. When cells were stained with an antibody to α_1-Pi (anti-α_1-Pi), finely granular deposits (but no globules) were observed. Staining was most intense in the pericentral (Rappaport zone 3) area, but occasional reactive cells were seen throughout the lobule.

The livers from the Z#1 lineage resembled those of the M#1 lineage, although

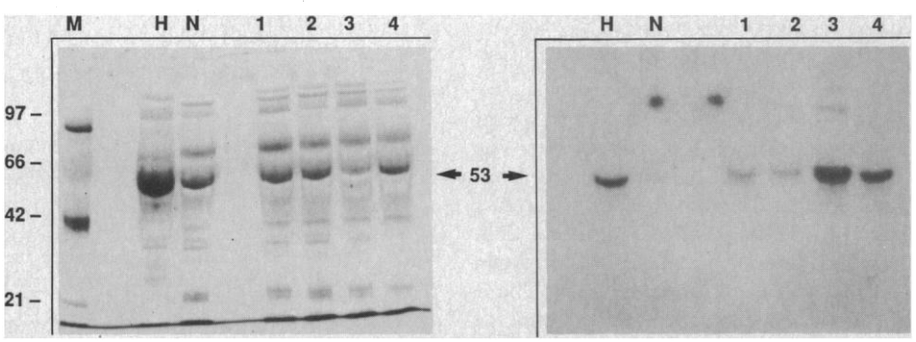

Fig. 3. An SDS-polyacrylamide gel of serum proteins (1 μl per lane). In the left panel the gel has been silver-stained. In the right panel, the gel has been immunoblotted and developed with a rabbit antibody to human α_1-Pi that had little cross-reactivity with mouse α_1-Pi and an iodinated donkey–anti-rabbit second antibody. Lane M represents size markers; sizes are shown in kilodaltons. Lane H is normal human serum and lane N is normal nontransgenic mouse serum. Lanes 1 to 4 are lineages Z#2, Z#1, M#1, and M#2, respectively.

hepatocytes were larger and binucleate cells were more frequently observed in Z#1. The α_1-Pi protein was seen as finely granular cytoplasmic material, particularly in pericentral hepatocytes, only after the PAP method was employed. Necrosis was not prominent.

In contrast, the Z#2 animals showed abundant α_1-Pi material that was easily seen in H-E sections as homogeneous eosinophilic globules of varying size, filling and distending obviously enlarged hepatocytes (Fig. 5A). The material reacted intensely with both dPAS (Fig. 5B) and anti-α_1-Pi (Fig. 5C), and was indistinguishable from that seen in human α_1-Pi deficiency except for the greater intensity of expression in the mouse model. Scattered individual cells, within a liver plate that was generally strongly reactive, were lacking globules with either dPAS or PAP tests (Fig. 5C). Microabscesses were seen that consisted of polymorphonuclear leukocytes and extracellular α_1-Pi material. The Z#2 lineage also showed irregular foci of liver cell necrosis, with formation of microcystic areas. Some of the microcystic areas contained red blood cells and resembled peliosis hepatitis. There were also separate focal accumulations of acute inflammatory cells, forming microabscesses. There was no fibrosis in any of the livers of 1-month-old animals, although there was regenerative activity as evidenced by multicellular liver plates and focal nodule formation in Z#2 animals. In addition, nodular clusters of altered hepatocytes lacking α_1-Pi material were also seen (Fig. 5C).

Alpha-1-Pi protein was found in other tissues besides liver. Chondrocytes, individual thymic epithelial cells and Hassall's bodies, macrophages in lymphoid tissue of the small intestine, gastric and small intestinal crypt epithelial cells, renal distal tubule brush border, and the material lining pulmonary alveoli (not visible in H-E sections) showed varying degrees of reactivity with dPAS and anti-α_1-Pi. Figure 5D shows two littermates. The larger animal is nontransgenic, the smaller animal is a Z#2 transgenic.

Three other groups have injected the human M allele α_1-Pi gene into mouse lineages (*11–13*). The consensus from these studies is that the α_1-Pi gene is expressed efficiently in the same tissues in which it is normally synthesized in humans. However, the protein is found in higher levels in mouse intestine than in human intestine. One group has commented on expression in cartilage (*14*). We have also seen high levels of protein in cartilage in all four transgenic lineages. Normal expression in cartilage has not been reported for mouse or human.

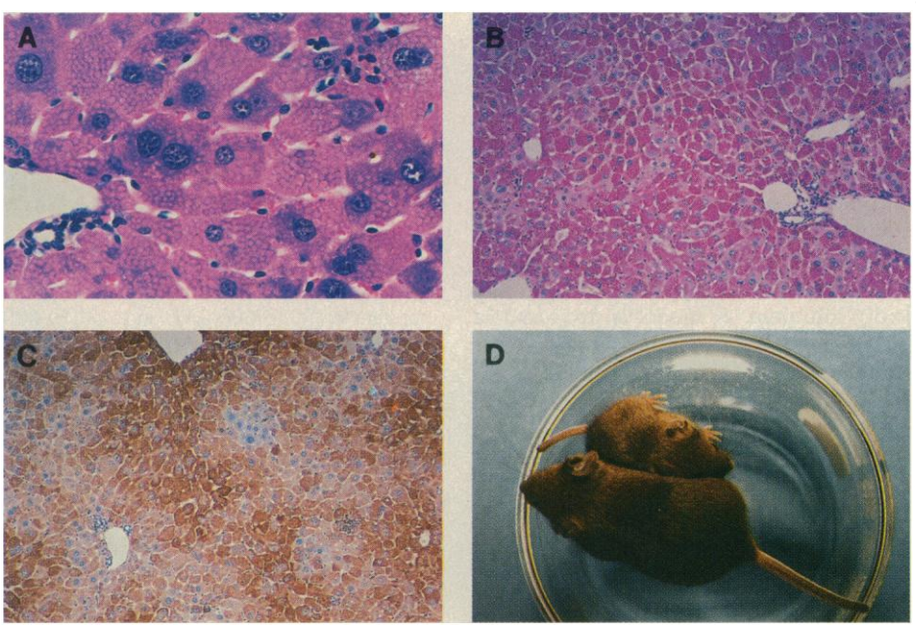

Fig. 5. (**A**) Hematoxylin-eosin stain of liver section. Liver section of a Z#2 transgenic reveals prominent distortion of the lobular pattern with widened liver plates and slight hepatocytic pleomorphism. The hepatocytes are distended by innumerable eosinophilic globules (×400). (**B**) Periodic acid–Schiff reaction on liver section after digestion with diastase (dPAS). Hepatocytes of Z#2 animals are packed with variably sized dPAS-positive cytoplasmic globules, most prominent in the peri-central (zone 3) region and the mid-lobular (zone 2) areas. Scattered regions of enlarged hepatocytes are almost completely free of dPAS-positive material (×100). (**C**) Hepatic section stained with rabbit anti-α_1-Pi by the PAP technique (rabbit primary antibody). Z#2 section shows most hepatocytes distended by α_1-Pi globular inclusions. Clusters of hepatocytes devoid of α_1-Pi globular inclusions and a typical microabscess are present (×100). (**D**) Two littermates at 3 weeks of age. The larger animal is not transgenic. The smaller animal is a Z#2 transgenic.

The human Z protein is not transported efficiently in *Xenopus* oocytes (*15, 16*). However, the nature of the transport defect is unknown; there might be a defective transport protein "receptor" or "channel," or there might be abnormal folding and precipitation or agglutination of the protein. Although the data presented here do not answer this question, the Z#2 mouse lineage should be a useful model to study the question.

The abnormalities of the Z#2 lineage closely resemble those observed in α_1-Pi–associated neonatal hepatitis in humans. Humans with α_1-Pi–associated neonatal hepatitis are small for gestational age (*5*) and do not gain weight during the first 2 months of life. Analogous to Z#2 mice, human neonates with hepatitis begin to gain weight by age 3 months, and reach normal size and weight by age 6 to 12 months (*5*). There is a possibility that the runting phenomenon seen in the Z#2 lineage is due, in part, to the site of integration of the human gene in the mouse chromosome. If the transgene were to disrupt an important gene for growth or development, then the transgenic animals could be defective in some important function. However, the fact that humans with the hepatic form of this disease are small for gestational age supports the hypothesis that runting is due to the liver involvement in the mice. We suspect that the Z#1 animals do not show the runting phenomenon because of the substantially lower levels of α_1-Pi RNA and protein found in their livers (Fig. 2). Our ability or inability to produce further founder strains with the runting phenomenon will lend strength to one or the other of the hypotheses.

We cannot explain the observation that the Z#2 transgenic animals are heterogeneous in weight during the first 3 months of life. Furthermore, we have not yet found an animal homozygous for the transgene. Since the animals are not inbred, being composed of C57BL/6J, CBA/J and some DBA/2J genetic information, there is a possibility that a second genetic locus is influencing the severity of the liver pathology and runting phenomenon. It will be necessary to backcross the transgenic animals to inbred strains to determine if any one of the parental lineages carries a gene that exacerbates the phenotype. We have also examined all animals for the presence of mouse hepatitis virus and have not found evidence of this virus in any one of the animals in the colony. Thus the best interpretaion of the current data is that the abnormal features of the Z#2 lineage can be ascribed to high level expression of the mutant α_1-Pi.

In summary, we have produced a new

transgenic mouse strain that displays many of the physical and histologic changes seen in human neonatal α_1-Pi disease. These animals are likely to be useful models for this human disease. In addition, the liver damage observed suggests that these animals may subsequently develop cirrhosis, and thus may also be useful in the study of this pathophysiologic state.

REFERENCES AND NOTES

1. J. Bieth, *Front Matrix Biol.* **6**, 1 (1978).
2. J. Jeppsson, *FEBS Lett.* **65**, 195 (1976).
3. L. Yoshida *et al.*, *Proc. Natl. Acad. Sci. U.S.A.* **73**, 1324 (1976).
4. F. Callea *et al.*, *J. Hepatol.* **2**, 389 (1986).
5. T. Sveger, *N. Engl. J. Med.* **294**, 1316 (1976).
6. R. W. Carrell and M. D. Owen, *Essays Med. Biochem.* **4**, 83 (1980).
7. J. R. Hodges *et al.*, *N. Engl. J. Med.* **304**, 557 (1981).
8. B. Hogan *et al.*, Eds., *Manipulating the Mouse Embryo: A Laboratory Manual* (Cold Spring Harbor Laboratory, Cold Spring Harbor, NY, 1986).
9. The original B6D2F2/J founder mice were backcrossed for one generation to C57Bl6/J mice. Female transgenic animals were then bred to B6XCBA F1 (C57Bl6/J × CBA) male animals, and single-cell embryos were transferred to pseudopregnant B6 × CBA F1 recipients. The resulting offspring represent the M#1, M#2, Z#1, and Z#2 "lineages".
10. M. J. Dycaico, K. Felts, and J. A. Sorge, unpublished data.
11. U. Ruther *et al.*, *Nucleic Acids Res.* **15**, 7519 (1987).
12. G. D. Kelsey *et al.*, *Genes Dev.* **1**, 161 (1987).
13. R. N. Sifers *et al.*, *Nucleic Acids Res.* **15**, 1459 (1987).
14. J. A. Carlson *et al.*, *J. Clin. Invest.* **82**, 26 (1988).
15. D. H. Perlmutter *et al.*, *Proc. Natl. Acad. Sci. U.S.A.* **82**, 6918 (1985).
16. D. M. Errington *et al.*, *Eur. J. Biochem.* **153**, 361 (1985).
17. E. Perlino *et al.*, *EMBO J.* **6**, 2767 (1987).
18. T. Maniatis *et al.*, Eds., *Molecular Cloning* (Cold Spring Harbor Laboratory, Cold Spring Harbor, NY, 1982).

19. Funded by contract #N01-HR-56024 from the National Heart, Lung and Blood Institute. We thank Z. Bengali for his encouragement and support as well as Y. Kim and P. Danao for outstanding histologic and immunohistochemical preparations.

19 May 1988; accepted 1 September 1988

Regulation of the Erythropoietin Gene: Evidence That the Oxygen Sensor Is a Heme Protein

MARK A. GOLDBERG, SUSAN P. DUNNING, H. FRANKLIN BUNN*

Erythropoietin (Epo), the hormone that stimulates red blood cell production, is synthesized in the kidney and liver in response to hypoxia. The human hepatoma cell line Hep3B regulates its production of Epo in a physiologic manner. Either hypoxia or cobalt chloride markedly increases expression of Epo mRNA as well as production of biologically active and immunologically distinct Epo protein. New protein synthesis is required before the induction of increased levels of hypoxia- or cobalt-induced Epo mRNA. Hypoxia, cobalt chloride, and nickel chloride appear to stimulate Epo production through a common pathway. The inhibition of Epo production at low partial pressures of oxygen by carbon monoxide provides evidence that a heme protein is integrally involved in the oxygen-sensing mechanism. This hypothesis is further supported by the finding that when heme synthesis is blocked, hypoxia-, cobalt-, and nickel-induced Epo production are all markedly inhibited. A model is proposed in which a ligand-dependent conformational change in a heme protein accounts for the mechanism by which hypoxia as well as cobalt and nickel stimulate the production of Epo.

ONE OF THE MAJOR UNANSWERED questions in the regulation of erythropoiesis is the mechanism by which hypoxia triggers the increased production of erythropoietin (Epo). In the fetus the liver is the primary site of Epo synthesis (*1*), whereas after birth, production shifts to the kidney (*2*). The lack of a cell culture system that produces readily measurable amounts of Epo in a regulated manner has hindered efforts to understand the intracellular and molecular events by which hypoxia induces increased production of Epo. We have reported that the human hepatoma cell line Hep3B increases its level of Epo mRNA and its production of Epo protein 20- to 50-fold in response to hypoxia and 6- to 12-fold in response to cobalt chloride (*3*). Using this cell culture system, we can now address questions regarding the nature of the oxygen sensor, which have been difficult to pursue with in vivo systems.

The existence of possible "second messengers" in the Epo regulatory pathway remains enigmatic. Androgens (*4*), prostaglandins (*5*), adenosine 3′,5′-monophosphate (cAMP) (*6*), and activated oxygen compounds (*7*) have all been proposed as intermediaries between stimulus and response. However, there is no consistent or convincing evidence that any of these substances act physiologically. Using the Hep3B cell culture system, we reported that prostaglandin E_2 had no effect on Epo production (*3*). We have now also investigated the effects of the calcium ionophore A23187 (0.1 to 5.0 μM), phorbol myristate acetate (10 to 100 nM), combinations of A23187 and phorbol myristate acetate, forskolin ($10^{-6}M$ to $10^{-4}M$), heat shock (42°C for 6 to 24 hours), hydrogen peroxide ($10^{-4}M$), triiodothyronine (1 to 10 nM), the potent calcium channel blocker lanthanum (1 mM), the androgens 5α-androstan-17β-ol-3-one ($10^{-7}M$ to $10^{-5}M$) and fluoxymesterone ($10^{-7}M$ to $10^{-5}M$), α-interferon (2×10^3 to 2×10^4 U/ml), adenosine ($10^{-8}M$ to $10^{-3}M$), and interleukin-1 (5 U/ml) on Epo production. None of these agents were active in inducing Epo protein synthesis in the Hep3B cell culture system.

Besides being stimulated by hypoxia, Epo production is reliably stimulated by the administration of cobalt. Cobalt increases the red cell mass in both man (*8*) and experimental animals (*9*). Experiments with intact animals (*9*) as well as perfused kidneys (*10*) have shown that cobalt stimulates erythropoiesis by increasing the production of Epo. However, the mechanism by which this response occurs is not understood. The suggestion (*11*) that cobalt acted through inhibition of cellular oxidative phosphorylation is not tenable, since more potent inhibitors of cell respiration, such as cyanide, have no effect on Epo production (*12*). Intrarenal injections of nickel also induce erythrocytosis (*13*). Hence, we incubated Hep3B cells for 24 hours in the presence of increasing concentrations of nickel chloride, and we observed a dose-dependent increase in Epo production to levels similar to those achieved with $CoCl_2$, albeit at a slightly higher molar concentration of nickel (Fig. 1). Subsequently, we studied the effects of manganese (50 to 600 μM), zinc (50 to 600 μM), iron (50 to 500 μM), cadmium (1 to 500 μM), and tin (10 to 100 μM) on Epo production by Hep3B cells. Of these elements only manganese induced measurable Epo levels, but these levels were less than those obtained by either cobalt or nickel (Fig. 1). Although cobalt, nickel, and manganese are not physiologic stimuli, information on their mechanism of action may provide insights into the regulation of Epo production.

To further delineate the nature of the oxygen-sensing mechanism in the Hep3B

Howard Hughes Medical Institute, Division of Hematology, Department of Medicine, Brigham and Women's Hospital, and Harvard Medical School, Boston, MA 02115.

*To whom correspondence should be addressed at Division of Hematology, Brigham and Women's Hospital, Boston, MA 02115.